J Fluoresc (2015) 25:577–583
DOI 10.1007/s10895-015-1537-x

ORIGINAL PAPER

Conformational Change Near the Redox Center of Dihydrolipoamide Dehydrogenase Induced by NAD^+ to Regulate the Enzyme Activity

Tomoe Fukamichi · Etsuko Nishimoto

Received: 19 December 2014 / Accepted: 20 February 2015 / Published online: 11 March 2015
© Springer Science+Business Media New York 2015

Abstract Dihydrolipoamide dehydrogenase (LipDH) transfers two electrons from dihydrolipoamide (DHL) to NAD^+ mediated by FAD. Since this reaction is the final step of a series of catalytic reaction of pyruvate dehydrogenase multi-enzyme complex (PDC), LipDH is a key enzyme to maintain the fluent metabolic flow. We reported here the conformational change near the redox center of LipDH induced by NAD^+ promoting the access of the DHL to FAD. The increase in the affinity of DHL to redox center was evidenced by the decrease in K_M responding to the increase in the concentration of NAD^+ in Lineweaver-Burk plots. The fluorescence intensity of FAD transiently reduced by the addition of DHL was not recovered but rather reduced by the binding of NAD^+ with LipDH. The fluorescence decay lifetimes of FAD and Trp were prolonged in the presence of NAD^+ to show that FAD would be free from the electron transfer from the neighboring Tyrs and the resonance energy transfer efficiency between Trp and FAD lowered. These results consistently reveal that the conformation near the FAD and the surroundings would be so rearranged by NAD^+ to allow the easier access of DHL to the redox center of LipDH.

Keywords Dihydrolipoamide dehydrogenase · FAD · NAD^+ · PDC · Time-resolved fluorescence

Abbreviations

LipDH	Dihydrolipoamide dehydrogenase
DHL	Dihydrolipoamide
FAD	Flavinadenine dinucleotide
NAD^+	Nicotineamide-adenine dinucleotide
RET	Resonance excitation energy transfer

T. Fukamichi · E. Nishimoto (✉)
Laboratory of Biophysical Chemistry, Faculty of Agriculture, Graduate School of Kyushu University, Fukuoka 812-8581, Japan
e-mail: enish@brs.kyushu-u.ac.jp

Introduction

Dihydrolipoamide dehydrogenase (LipDH) is one component of pyruvate dehydrogenase multi- enzyme complex (PDC) and contributes to the retaining of the physiological functions of PDC by co-operating synchronously with the pyruvate decarboxylase and lipoamide acetyltransferase. PDC connects glycolysis pathway and TCA cycle and is, therefore, indispensable for the fluent energy and material metabolism of both of prokaryotic and eukaryotic cells. LipDH plays the most important part in a series of catalytic reaction chain of PDC by completing final step. In fact, it is known that the deficiency of LipDH causes the development of lactic acidosis and neurological degeneration [1–5].

The over-all reaction catalyzed by LipDH is described as

$$\text{Dihydrolipoamide} + NAD^+ \rightarrow \text{Lipoamide} + NADH + H^+$$

The redox center of LipDH is constructed by the combination of a disulfide bridge coupled to the flavin ring of FAD. The two electrons of dihydrolipoamide (DHL) are transferred to the disulfide bridge mediated by FAD and then, FAD is reduced to $FADH_2$. The reduced form of FAD, $FADH_2$ is formed transiently in the first half-reaction of LipDH and oxidized back to FAD by reducing NAD^+ to NADH in the latter half-reaction. Flavin moiety of FAD displays a peculiar fluorescence property. The reduced form of FAD is non-fluorescent in spite that the flavin molecule itself emits

appropriate fluorescence around 530 nm for the conditions. This specific fluorescence property is expected to be useful to examine the catalytic and regulation mechanism of LipDH because non-fluorescent $FADH_2$ closely involves with the enzymatic reaction of LipDH [6]. FAD has been frequently employed as the useful intrinsic fluorescence probe to reveal subtle conformational changes and dynamics in some flavoproteins [7, 8]. The excited singlet state of FAD is so sensitive to the interactions with surrounding amino acid residues such as the electron transfer and the resonance excitation energy transfer.

In the present study, we investigated the regulation mechanism of the catalytic reaction of LipDH from *Bacillus Stearothermophilus*. The X-ray structure of LipDH is confirmed within 2.5 Å resolution. As shown in Fig. 1, LipDH adopts the dimeric form and single FAD is non-covalently arranged in each sub-unit. According to Mande, each sub-unit is composed of FAD-binding, central and interface domain in many kind of dihydrolipoamide dehydrogenase (not shown in Fig. 1) [9]. The location of FAD would be considered to be the just adjacent part to the interface domain. Furthermore, FAD is surrounded with some tyrosine residues and single Trp which would affect the fluorescence properties of LipDH. The catalytic reaction of LipDH has been well elucidated through many structural studies [10]. However, PDC especially, LipDH maintains the specific catalytic reaction mode to complete the determinant role in metabolic system for life. Therefore, more detailed studies on the multiple regulation mechanisms of LipDH, some of which are still unknown, are required.

In the present study, we investigated the conformational change near the redox center which closely associated to the regulation of LipDH of *B. stearothermophilus* noting the specific fluorescence properties of FAD.

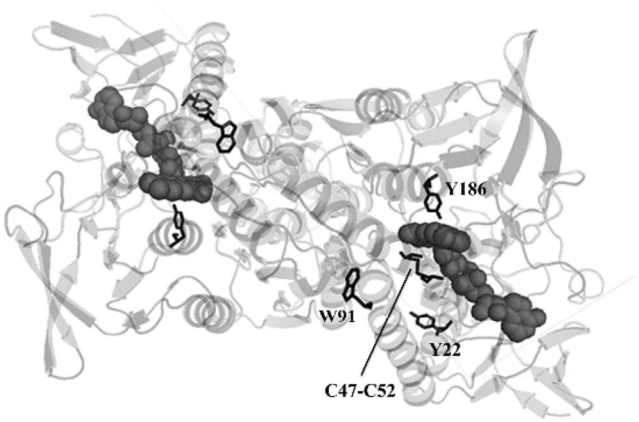

Fig. 1 The crystal structure of dihydrolipoamide dehydrogenase from *Bacillus stearothermophylus* (PDB accession code, 1EBD). FAD was represented by the dark circle and disulfide bridge, Tyr186, Tyr22 and Trp91 in each sub-unit were indicated by *thick lines*. The structure was drawn using PyMOL software

Materials and Methods

Chemicals

Dihydrolipoamide dehydrogenase (LipDH) from *B. stearothermophilus* was purchased from Unitika Ltd (Osaka, Japan). Alfa-Lipoamide, NAD^+ and other reagents for the buffer system (Sigma, St Lois, MO) were of special grade and used without further purification.

Purification of LipDH

LipDH with purity of more than 90 % was further purified by anion-exchange and gel-filtration chromatography. LipDH dissolved in the 20 mM phosphate buffer (pH 7.0) including 2 mM EDTA was applied to HiTrap Q HP column (GE Healthcare, UK). The purified LipDH was recovered as a single band in the 0.1–0.6 M NaCl gradient. LipDH sample used for the measurement was finally obtained by the PD-10 gel-filtration column (GE Healthcare, UK). Every purification by chromatography is performed on Duo-Flow system (Bio-Rad Laboratories, Inc. Hercules, CA). The purity of LipDH was confirmed by a beautiful single band corresponding to MW=110,000 on the native PAGE. The concentration of LipDH was determined photometrically and adjusted to be 0.5 mM through the present studies.

Preparation of DHL

DHL was prepared from α-lipoamide based on the method of Reed et al. [11]. Alfa-lipoamide dissolved in the cold water (20 %) – methanol (80 %) solution was mixed with the aqueous solution of $NaBH_4$ and incubated for 45 min until the solution was transparent. After acidification by dilute HCl, DHL was extracted by chloroform. The obtained DHL was purified by recrystallization method using mixed solvent including benzene and hexane at the ratio of 5:2.

Enzymatic Activity of LipDH

The enzyme activity was estimated by measuring increase in the absorption at 340 nm caused by the produced NADH from NAD^+. The measurement of the absorption is started just after mixing of LipDH with two substrates, DHL and NAD^+, in the 20 mM phosphate buffer (pH 7.0) including 2 mM EDTA, 1 mM $MgCl_2$ and 0.1 mM TPP. While the absorption at 340 nm increased single-exponentially, the initial increment was measured as the NAD^+ reducing reaction velocity. The Lineweaver-Burk plot,

$$\frac{1}{v} = \frac{1}{V_{\max}} + \frac{K_M}{V_{\max}} \frac{1}{[S]} \quad (1)$$

where, v was reaction velocity; V_{max}, maximum velocity; K_M, Michaelis constant; [S], concentrations of substrates, was used for the determination of K_M. The measurement of absorption was performed using Ultrospec3100pro spectrophotometer (GE healthcare).

Steady-State Fluorescence

The steady-state fluorescence spectrum was measured by Hitachi F-3010 fluorescence spectrophotometer (Tokyo, Japan). The emission spectra were corrected against the excitation and detection system. The undesired effects caused by the scattering and stray light were removed using subtraction program.

The time-trajectory of the fluorescence intensity during the enzymatic reaction of LipDH was traced by the same spectrophotometer. The excitation and emission wavelengths were 480 and 530 nm, respectively.

Time-Resolved Fluorescence Measurements

The fluorescence intensity was measured using sub-picosecond laser-based time-correlated single photon counting (TCSPC) method. The excitation pulse was separated from the combination of sub-picosecond laser (TSUNAMI, Spectra-Physics, Mountain View, CA), second harmonics generator/pulse selector (model 3980, Spectra-Physics) and third harmonics generator (GWU, Spectra-Physics). The excitation pulse and the fluorescence were detected with avalanche photodiode (C5658, Hamamatsu Photonics, Shizuoka, Japan) and MCP-photomultiplier (3809U-50, Hamamatsu Photonics), respectively. The outputs of the time-to-amplitude converter (TAC457, Ortec, Oak Ridge, TN) were accumulated in 2048 channels of MCA (Maestro-32, Ortec). The fluorescence decay was given by the liner combination of exponentials,

$$F(t) = \sum \alpha_i \exp\left(-t \Big/ \tau_i\right) \quad (2)$$

where τ_i was i-th decay time and α_i the corresponding pre-exponential factor. The decay kinetics and parameters α_i and τ_i were decided by the convolution-nonlinear least square methods based on the Marquardt algorism [12, 13]. The adequacy of the decay parameters were judged by σ, serial variance ratio (SVR) and weighted residuals. The values giving σ <1.2 and SVR>1.8 were adopted as the adequate α_i and τ_i. The details used for the measurement of the time-resolved fluorescence were described in Ref. [14].

Results and Discussion

LipDH catalyzes the reduction of NAD^+ by DHL mediated by the redox center composed of FAD and disulfide bridge. Therefore, the over-all enzymatic activity can be estimated by measuring the NADH producing rate. When Lineweaver-Burk plots were examined measuring the initial increment of the absorption at 340 nm, beautiful liner relationship was recognized between the reciprocals of enzymatic velocity and the substrate concentration in the LipDH solutions including various concentrations of DHL and NAD^+. One example including 2.5 mM NAD^+ was shown in the insert of Fig. 2. K_M values for LipDH against DHL estimated by the intercept and slope of the liner line in Lineweaver-Burk plots decreased with increasing in the concentration of NAD^+ as shown in Fig. 2. This result suggests that the affinity of LipDH to DHL would be enhanced in the presence of NAD^+.

Enzymatic reaction of LipDH is mediated by FAD which works as the redox center and FAD shuttles between two states during the enzymatic reaction. The reduced form of FAD, $FADH_2$ is non-fluorescent. $FADH_2$ is formed as the enzymatic reaction intermediate in the presence of DHL and absence of NAD^+. The fluorescence of FAD in LipDH from *Bacillus stearothermophilus* is not so strong, but the emission centered at 530 nm could be observed when excited at 480 nm.

When DHL was added to the buffer solution including LipDH in the absence of NAD^+, the fluorescence intensity of FAD decreased gradually with the time to reach to the constant value as shown in Fig. 3. The fluorescence decrease was not dependent on the concentration of the added DHL in

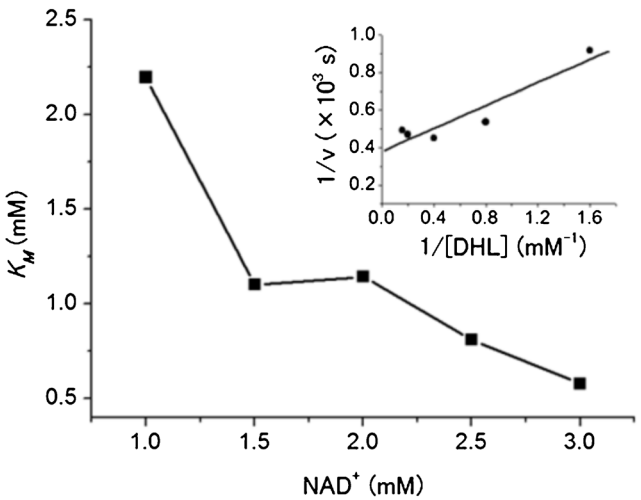

Fig. 2 NAD^+ dependence of K_M in the ezymatic reaction of LipDH against DHL. K_M was evaluated in the Lineweaver-Burk plot against DHL in the presence of various concentration of NAD^+. The concentration of LipDH was 0.5 mM. Insert, Lineweaver-Burk plot for LipDH against DHL in the presence of 20 mM NAD^+. v was estimated initial increment of the absorption at 340 nm caused by the production of NADH

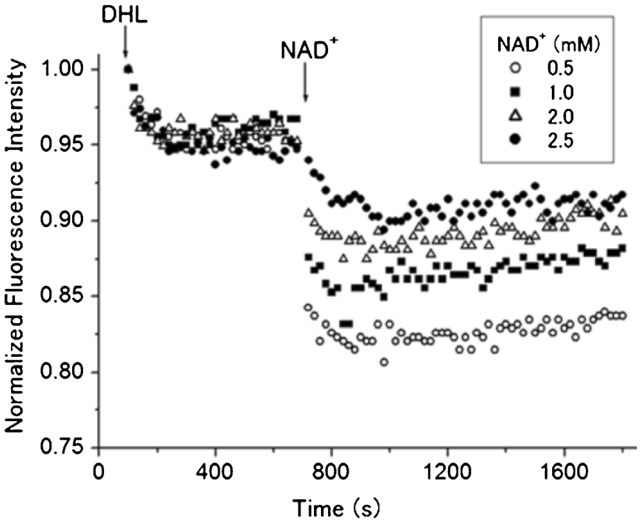

Fig. 3 The time-trajectory of the fluorescence intensity change of FAD induced by DHL and NAD^+. The added concentration of DHL was 0.65 mM. The final concentrations of the added NAD^+ were shown in the figure. The concentration of LipDH was 0.5 mM in the 20 mM phosphate buffer (pH 7.0). The excitation and emission wavelengths were 480 and 530 nm, respectively

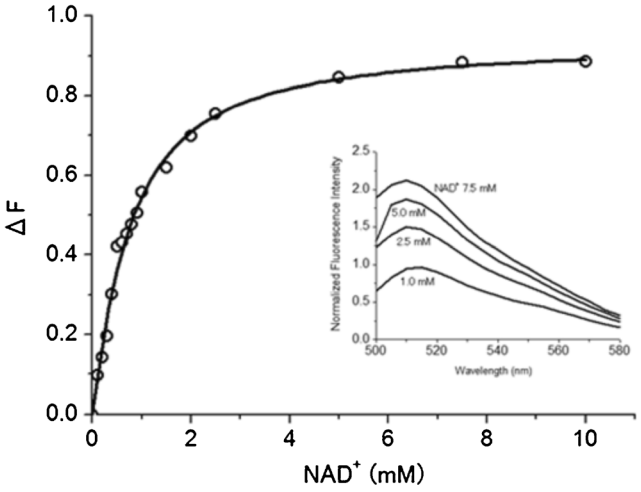

Fig. 4 Hill plots for the binding of LipDH with DHLip. The increment of the fluorescence intensity created by NAD^+ was plotted based on the Hill equation, $\Delta F = \frac{\Delta F_{\max}[NAD^+]^n}{K_d^n + [NAD^+]^n}$, where $\Delta F_{\max}$ was the maxim value of the fluorescence intensity change, K_d, the dissociation constant and n co-operative index. The concentration of LipDH was 0.5 mM in the 20 mM phosphate buffer (pH 7.0). The excitation and emission wavelengths were 450 and 530 nm, respectively. Insert, the fluorescence spectral change of LipDH induce by NAD^+. The added concentration of NAD^+ was shown in the figure

the range of 0.6–3.0 mM to suggest that LipDH would be saturated with DHL. This decrease in the fluorescence of FAD must be due to the change of FAD to $FADH_2$. When NAD^+ was added after the fluorescence intensity reach to the constant, it is expected that the fluorescence intensity would be recovered because of the conversion of $FADH_2$ to FAD by the reduction of NAD^+ to NADH. However, the fluorescence of FAD was rapidly decreased further just after the addition of NAD^+ and then increased slowly as shown in Fig. 3. The fluorescence decreases by the addition of NAD^+ was larger and more rapid as the concentration of NAD^+ was lower. (Data is not shown) This surprising observation demonstrates that the binding of NAD^+ with LipDH would promote the preceding half-reaction of LipDH with DHL. The reaction of LipDH with DHL to reduce FAD to $FADH_2$ would compete with the NAD^+ reducing (FAD reproducing) reaction. In the presence of the higher concentration of DHL and NAD^+, conversion rate of $FADH_2$ to FAD also becomes higher. Therefore, the decrease in the fluorescence of LipDH by addition of NAD^+ would be cancelled with the formation and consume of $FADH_2$ in the presence of higher concentration NAD^+.

The fluorescence of LipDH was enhanced by the presence of NAD^+. As shown in Fig. 4, the fluorescence was increased almost two times by the presence of 10 mM NAD^+ without any spectral shift. The titration curve of the fluorescence increment against the concentration of NAD^+ showed the excellent fit to the Hill equation,

$$\Delta F = \frac{\Delta F_{\max}[NAD^+]^n}{K_d^n + [NAD^+]^n} \quad (3)$$

where ΔF, ΔF_{max}, K_d, and n were the fluorescence increment by the addition of NAD^+, the maximum increment, the dissociation constant and co-operative index, respectively. The results of curve fitting with precision more than 99 % demonstrated that the sub-unit of LipDH bound with NAD^+ at molecular ratio 1:1 and the dissociation constant was 0.74 mM.

The fluorescence decay profiles of LipDH excited at 430 nm were shown in Fig. 5. It was clearly seen that the fluorescence of FAD decayed more slowly by the binding

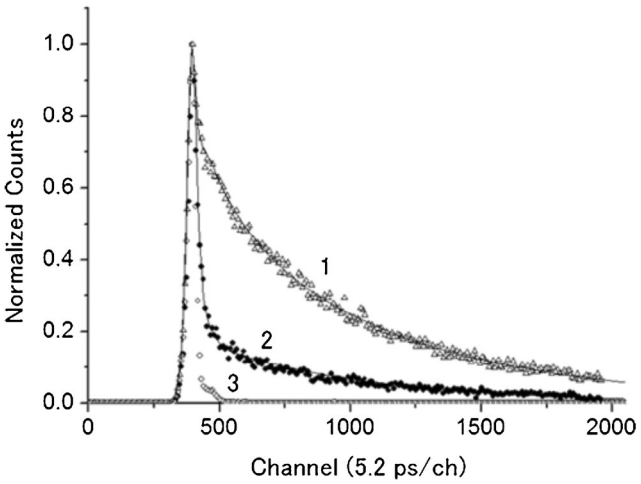

Fig. 5 The fluorescence intensity decay of FAD on the excitation at 430 nm. Curve 1, 2 and 3 were fluorescence decay of LipDH in the presence of 15 mM NAD^+, LipDH and the instrumental response function (IRF), respectively. The *solid lines* were drawn using the decay parameters giving the best fit. The emission wavelength was 530 nm. Channel width was 5.2 ps/channel

Table 1 Fluorescence decay parameters of FAD in LipDH

	α_1	α_2	α_3	τ_1(ns)	τ_2(ns)	τ_3(ns)	τ_{ave}(ns)	σ	SVR
E_3	0.94	0.06	–	0.08	3.14	–	0.25	1.10	1.18
E_3+NAD$^+$	0.87	0.09	0.05	0.02	3.75	0.79	0.39	1.06	1.80

Excitation wavelength, 430 nm. Emission wavelength, 530 nm

Table 2 Fluorescence decay parameter of Trp91 in LipDH

	α_1	α_2	τ_1(ns)	τ_2(ns)	τ_{ave}(ns)	σ	SVR
E_3	0.62	0.38	0.20	1.55	0.71	1.09	1.81
E_3+NAD$^+$	0.69	0.31	0.47	2.65	1.15	1.07	1.80

Excitation wavelength, 295 nm. Emission wavelength, 340 nm

with NAD$^+$. The fluorescence decay parameters in the presence and absence of NAD$^+$ were summarized in Table 1. The fluorescence decay kinetics of LipDH was changed from double-exponential to triple-exponential and the contribution of the component with the longest decay time to the total emission was increased by the binding with NAD$^+$. Consequently, the average lifetime was prolonged from 0.20 to 0.39 ns to suggest that the interactions with the surrounding amino acid residue to quench the fluorescence of FAD would be suppressed. According to van der Berg et al. and Yang et al., the electron transfer from Tyr residue most contributes to the fluorescence quenching of FAD in many flavoproteins [15, 16]. Two tyrosine residues, Tyr186 and Tyr22, locate at the side where the NAD$^+$ binding site is arranged against FAD and at the opposite side, respectively. These two Tyrs doubtlessly quench the fluorescence of FAD in LipDH. Especially, the quenching rate by Tyr186 which locates at the same side to NAD$^+$ binding pocket would be larger because Tyr186 is very close to flavin ring. Since the electron transfer rate from Tyr to FAD is given by the exponential of the electron donor- acceptor distance, the probability of the quenching by Tyr22 which locate 14.6 Å apart from FAD must be not so lower. Our experimental results demonstrate that the binding of NAD$^+$

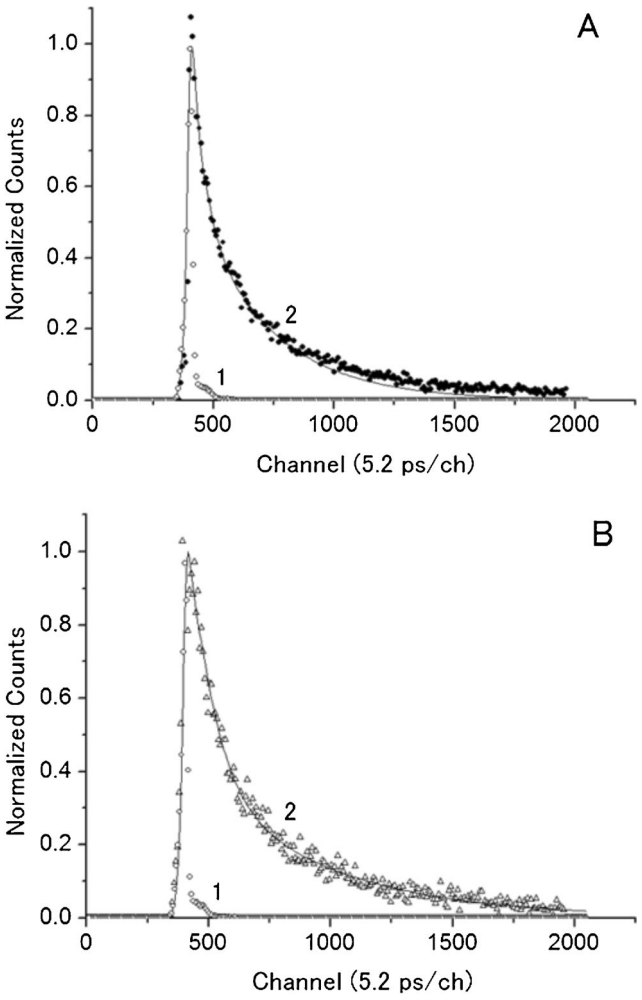

Fig. 6 The fluorescence intensity decay of Trp91. *Panel A* and *B* were the fluorescence of LipDH in the absence and presence of 15 mM of NAD$^+$, respectively. The excitation wavelength was 295 nm and the emission was measured at 340 nm. Channel width was 5.2 ps/channel. Curve 1 was IRF, and Curve 2, the fluorescence of Trp91 in each panel. The *solid lines* for the fluorescence decay were drawn by using the parameters giving the best fit

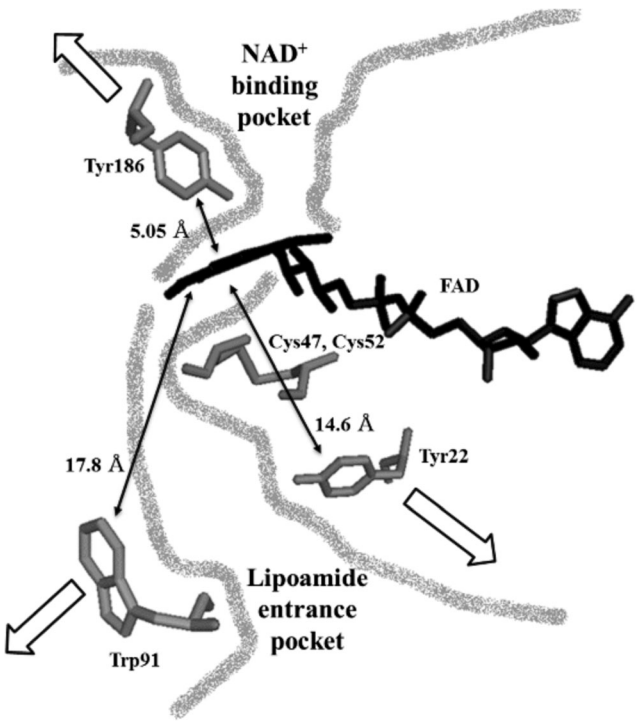

Fig. 7 The conformational change near the redox center of LipDH. The redox center composed of the FAD and disulfide bridge separates the NAD$^+$ binding pocket from DHL entrance pocket [21]. The distance between Tyr186, Tyr22 and Trp91 were indicated in the figure based on the X-ray structure. The conformation changes of Tyr186, 22 and Trp91 surrounding the redox center were shown by the *arrows* in the figure

moves away of Tyr186 and also extends the distance between FAD and Tyr22. The similar NAD^+ binding effect were recognized in the crystal structure analysis of some other flavoproteins such as glutathione reductase and LipDH from *Pseudomonas putida* [17, 18].

The resonance excitation energy transfer (RET) is generally known between Trp and FAD and it is also confirmed that the critical distance is 20 Å [19]. The sub-unit of LipDH is a single Trp containing protein and Trp91 locates near the entrance pocket of DHL of LipDH where is the opposite side to the NAD^+ binding site against the isoalloxazine ring of FAD. The fluorescence decay of Trp91 was measured on the excitation at 295 nm to examine the NAD^+ binding effects. The fluorescence decay profiles of Trp91 and the decay parameters were shown in Fig. 6 and Table 2, respectively. The fluorescence decay kinetics was the double-exponential which was probably ascribed to the heterogeneity of the conformation surrounding Trp91. Corresponding to the slower decay seen in the figure, the decay times of each component and average lifetime of Trp91 were prolonged by the binding of NAD^+. This result suggests that the energy transfer rate was reduced between Trp91 and flavin ring of FAD because the fluorescence decay times of the energy donor (Trp91) were prolonged. It may be difficult to consider that the non-radiative transition rate of Trp91 would be almost due to the energy transfer to FAD. However, it was shown in the unfolding intermediate studies that the energy transfer efficiency from Trp91 to FAD changed in responding to the structural shrink and/or relaxation of the tertiary structure of LipDH [20]. Therefore, it would be not unreasonable to conclude that Trp91 would change the location apart from FAD by the binding of NAD^+ with LipDH. The relations during the fluorescence energy transfer efficiency (E), distances (r) and fluorescence decay times are generally known,

$$E = 1 - \frac{\tau_{DA}}{\tau_D} \tag{4}$$

$$E = \frac{R_0^6}{R_0^6 + r^6} \tag{5}$$

where, τ_{DA} and τ_D are fluorescence lifetimes of the donor in the presence and absence of the acceptor, respectively and R_0 the critical distance. Using these relations, the change in the distance between Trp91 and FAD could be estimated because it is known that Trp91 locates about 17.8 Å apart from flavin ring. Responding to the binding of NAD^+, Trp91 moved almost 2.5 Å to the distant direction from flavin ring.

Conclusion

The decrease in K_M in enzymatic reaction of LipDH against DHL by increasing in the NAD^+ concentration and the rapid decreases of the fluorescence intensity by addition of NAD^+ after the completing the first half-reaction demonstrated that the approach of DHL to the redox center would be accelerated by the NAD^+. On the other hand, the NAD^+ binding effect on the fluorescence decays of FAD and Trp91 would give the structural basis for it. As seen in the structure of LipDH from *B. stearothermophilus* schematically represented in Fig. 7 based on the X-ray analysis, the isoalloxazine ring of FAD separate the NAD^+ binding site from the DHL entrance pocket. The disulfide bridge is adjacent to the isoalloxazine ring and Trp91 and Tyr22 are arranged in the DHL entrance pocket. On the other hand, Tyr186 occupies a position at the opposite side against the isoalloxazine ring. Our experimental results showed that Tyr186, 22 and Trp91 removed away from FAD by the binding of NAD^+ to secure the certain space. Such conformational change would make the approach of DHL to redox center easier to accelerate the preceding half-reaction of ping-pong catalytic reaction of LipDH.

References

1. Hong YS, Kerr DS, Liu T-C, Lusk M, Powell BR, Patel MS (1997) Deficiency of dihydrolipoamide dehydrogenase due to two mutant alleles (E340K and G101del): analysis of a family and prenatal testing. Biochim Biophys Acta 1362(2–3):160–168
2. Robinson BH, Taylor J, Sherwood WG (1977) Deficiency of dihydrolipoyl dehydrogenase (a component of the pyruvate and α-ketoglutarate dehydrogenase complexes): a cause of congenital chronic lactic acidosis in infancy. Pediatr Res 11:1198–1202
3. Elpeleg ON, Saada AB, Shaag A, Glustein JZ, Ruitenbeek W, Tein I, Halevy J (1997) Lipoamide dehydrogenase deficiency: a new cause for recurrent myoglobinuria. Muscle Nerve 20(2):238–240
4. Berger I, Elpeleg ON, Saada A (1996) Lipoamide dehydrogenase activity in lymphocytes. Clin Chim Acta 256(2):197–201
5. Sakaguchi Y, Yoshino M, Aramaki S, Yoshida I, Yamashita F, Kuhara T, Matsumoto I, Hayashi T (1986) Dihydrolipoyl dehydrogenase deficiency: a therapeutic trial with branched-chain amino acid estriction. Eur J Pediatr 145(4):271–274
6. Lu HP, Xun L, Xie XS (1998) Single-molecule enzymatic dynamics. Science 282:1877–1882
7. van den Berg PAW, Feenstra KA, Mark AE, Berendsen HJC, Visser AJWG (2002) Dynamic conformations of flavin adenine dinucleotide: Simulated molecular dynamics of the flavin cofactor related to the time-resolved fluorescence characteristics. J Phys Chem B 106: 8858–8869
8. Liu T-C, Hong YS, Korotchkina LG, Vettakkorumakankav NN, Patel MS (1999) Site-directed mutagenesis of human dihydrolipoamide dehydrogenase: role of lysine-54 and glutamate-192 in stabilizing the thiolate-FAD intermediate. Protein Expr Purif 16:27–39
9. Mande SS, Sarfaty S, Allen MD, Perham RN, Hol WG (1996) Protein-protein interactions in the pyruvate dehydrogenase multienzyme complex: dihydrolipoamide dehydrogenase complexed with

the binding domain of dihydrolipoamide acetyltransferase. Structure 4:277–286
10. Williams CHJ (1992) Lipoamide dehydrogenase, glutathione reductase, thioredoxin reductase, and mercuric ion reductase-a family of flavoenzyme transhydrogenases. In: Müller F (ed) Chemistry and biochemistry of flavoenzymes, vol 3. CRC Press, Boca Raton, pp 121–211
11. Reed LJ, Koike M, Levitch ME, Leach FR (1958) Studies on the nature and reactions of protein-bound lipoic acid. J Biol Chem 232: 143–158
12. Willis KJ, Szabo AG (1989) Resolution of tyrosyl and tryptophyl fluorescence emission from subtilisins. Biochemistry 28(11):4902–4908
13. Zuker M, Szabo AG, Bramall L, Krajcarski DT, Selinger B (1985) Delta function convolution method (DFCM) for fluorescence decay experiments. Rev Sci Instrum 56(1):14–22
14. Nakashima H, Fukunaga Y, Ueno R, Nishimoto E (2014) Sugar binding effects on the enzymatic reaction and conformation near the active site of pokeweed antiviral protein revealed by fluorescence spectroscopy. J Fluoresc 24(3):951–958
15. van den Berg PAW, van Hoek A, Walentas CD, Perham RN, Visser AJWG (1998) Flavin fluorescence dynamics and photoinduced electron transfer in *Escherichia coli* glutathione reductase. Biophys J 74:2046–2058
16. van den Berg PAW, van Hoek A, Visser AJWG (2004) Evidence for a novel mechanism of time-resolved flavin fluorescence depolarization in glutathione reductase. Biophys J 87(4):2577–2586
17. Mattevi A, Obmolova G, Sokatch JR, Betzel C, Hol WGJ (1992) The refined crystal structure of *Pseudomonas putida* lipoamide dehydrogenase complexed with NAD^+ at 2.45 Å resolution. Proteins Struct Funct Genet 13:336–351
18. D'Anna JA, Tollin G (1971) Protein fluorescence and solvent perturbation spectra as probes of flavin-protein interactions in the Shethna flavoprotein. Biochemistry 10:57–64
19. Nishimoto E, Aso Y, Koga T, Yamashita S (2006) Thermal unfolding process of dihydrolipoamide dehydrogenase Studied by fluorescence spectroscopy. J Biochem 140(3):349–357
20. Ghisla S, Massey V (1989) Mechanisms of flavoprotein-catalyzed reactions. Eur J Biochem 181(1):1–17
21. Yang H, Luo G, Karnchanaphanurach P, Louie T-M, Rech I, Cova S, Xun L, Xie XS (2003) Protein conformational dynamics probed by single-molecule electron transfer. Science 302:262–266